MATHEMATICAL ENGINEERING TECHNICAL REPORTS

Stabilization of Multi-agent Dynamical Systems for Cyclic Pursuit Behavior

Tae-Hyoung KIM, Shinji HARA and Yutaka HORI

(Communicated by Kazuo MUROTA)

Stabilization of Multi-agent Dynamical Systems for Cyclic Pursuit Behavior

Tae-Hyoung KIM*, Shinji HARA and Yutaka HORI†

October 27th, 2009

Abstract

This paper studies pursuit formation stabilization problem in target-enclosing operations by multiple homogeneous dynamic agents. To this end, we first present Lyapunov and asymptotic stability conditions which should hold for the on-line path generation laws. The formation control scheme combined with a cyclic pursuit based distributed on-line path generator satisfying the derived stability conditions guarantees the required global convergence property with theoretical rigor. Next, based on the above results, we introduce a $\mathcal{D}$-stability problem by considering the requirements for multi-agent system's transient performance, and then develop a simple diagrammatic pursuit formation stability criterion. Then, as for the formation stabilization problem when agent's dynamics and its local controller are given, we develop an optimization problem subject to LMI constraints derived based on the generalized Kalman-Yakubovich-Popov (GKYP) lemma to maximize the connectivity gain of a cyclic pursuit based on-line path generator. It provides a permissible range of gain, which guarantees the satisfaction not only of a global formation stability condition but also of a required performance specification. Finally, a constrained polynomial optimization problem is developed, in order to design agent's local controller parameters guaranteeing that a connectivity gain becomes the maximum one satisfying the global formation stability condition for a class of dynamic agents given a priori. Several examples are given to illustrate its distinctive features and the achievement of a desired pursuit pattern.

Keywords: Multi-agent systems; Cooperative control; Distributed control; Pursuit problems; Circulant matrices; Generalized Kalman-Yakubovich-Popov (KYP) lemma; Linear matrix inequality (LMI)

---

*School of Mechanical Engineering, Chung-Ang University, 221 Heukseok-dong, Dongjak-gu, Seoul 156-756, Korea. E-mail: `kimth@cau.ac.kr`

†Department of Information Physics and Computing, Graduate School of Information Science and Technology, The University of Tokyo, 7-3-1 Hongo, Bunkyo-ku, Tokyo 113-8656, Japan. E-mail: {`Shinji_Hara,Yutaka_Hori`}@ipc.i.u-tokyo.ac.jp

1 Introduction

Formation control which coordinates the motion of relatively simple and inexpensive multiple agents is one of the essential technologies that enable agents to cover a larger operational area and achieve complex tasks (see [14, 13, 2] and the references therein). Several research groups recently developed coordination control strategies which achieve an enclosing formation around a specific area (object) by multiple agents using local information [10, 9, 11, 15, 5].

Recently, Kim and Sugie [8] proposed a distributed on-line path planning method for target-enclosing operations by multi-agent systems based on a modified cyclic pursuit strategy. Despite its simple but particularly effective nature for target-enclosing tasks, it could be a considerable drawback in real implementations that each agent is assumed to be a point mass with full actuation. That is, since agent's dynamics is not explicitly considered in path planning, their approach may suffer from the potential problem that each agent cannot precisely track its designed trajectory. In this case, the global convergence of multiple agents to the designated formation may not be achieved. In order to overcome the above difficulties, Kim et al. [7] recently developed a distributed pursuit cooperative control scheme for multiple dynamic agents, and then presented a simple diagrammatic formation stability analysis method based on the results given in Hara et al. [3].

In this paper, we consider multiple agents in 3D space, which have common system dynamics and identical local controllers. For such multi-agent dynamical systems, this paper proposes optimization-based formation stabilization strategies for a distributed cooperative control for target-enclosing operations based on a cyclic pursuit scheme. To this end, we first summarize the following conventional results presented by Kim et al. [7] in Sections 4-5: a formation stability analysis of distributed cooperative control for target-enclosing operations by multiple homogeneous dynamic agents. Next, we introduce a $\mathcal{D}$-stability problem by considering the requirements for the above multi-agent system's transient performance, and develop the diagrammatic pursuit formation $\mathcal{D}$-stability criterion at the end of Section 5. Then, based on the above results, the following two kinds of optimization problems for a pursuit formation stabilization are considered:

[Problem S1] *Maximization of a connectivity gain of a cyclic pursuit based on-line path generator, which satisfies for given agent's dynamics and its local controller not only a global formation stability condition but also a required multi-agent system's performance specification.*

[Problem S2] *Optimization of agent's local controller parameters for a class of agent's dynamics given a priori, so that a given connectivity gain becomes the maximum one guaranteeing the global pursuit formation stability.*

In order to derive an optimization problem for "Problem S1", we first show that the required pursuit formation stability condition can be converted to the linear matrix inequalities (LMIs), which are numerically tractable and can be solved efficiently, based on the generalized Kalman-Yakubovich-Popov (GKYP) lemma [4, 6]. Then, a concrete optimization problem subject to LMI constraint conditions for maximizing the connectivity gain, which satisfies the requirements given in "Problem S1", is developed in Section 6. Further, in order to clearly show its distinctive features, the special case such as an optimization-based pursuit formation stabilization scheme for a class of multi-agent dynamical systems combined with PID controllers is presented in Section 7.2. Finally, we develop a constrained polynomial optimization problem to solve "Problem S2" in Section 8. It provides a considerably simple and systematic optimization-based local PD controller design method, which guarantees the global pursuit formation stability of a considered multi-agent dynamical system. Several numerical examples illustrate its distinctive features and the achievement of a desired pursuit pattern.

The following notations will be used hereafter: For a Hermitian matrix, $M > 0$, $M \geq 0$, $M < 0$, and $M \leq 0$ denote positive definiteness, positive semidefiniteness, negative definiteness, and negative semidefiniteness, respectively. The transpose and complex conjugate transpose of the matrix M are denoted by M^T and M^*, respectively. The symbol $\mathbf{H}_n$ denotes the set of $n \times n$ Hermitian matrices. The Kronecker product of matrices Γ and P is $\Gamma \otimes P$. The real and imaginary parts of a complex variable z is represented by $\mathrm{Re}[z]$ and $\mathrm{Im}[z]$, respectively.

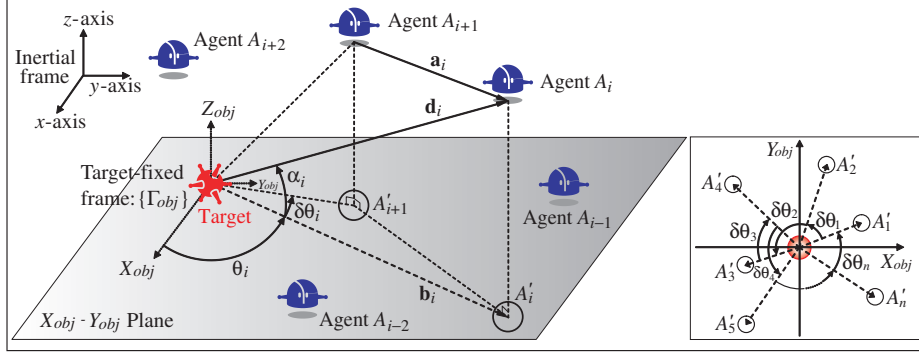## 2   System description and control aim

Consider a group of n agents dispersed in 3D space as shown in Figure 1(a). All agents are ordered from 1 to n; i.e., A_1, $A_2, \cdots, A_n$. We define A_{i+1} as prey agent of $A_i{}^1$. Denote the position vectors of the stationary target object and the moving agent A_i $(i = 1, 2, \cdots, n)$ in the inertial frame by $\boldsymbol{x}_o \in \mathbb{R}^3$ and $\boldsymbol{x}_i(t) \in \mathbb{R}^3$, respectively. It is assumed that an agent A_i can measure the following vectors:

$$\mathbf{d}_i := \boldsymbol{x}_i - \boldsymbol{x}_o, \quad \boldsymbol{a}_i := \boldsymbol{x}_i - \boldsymbol{x}_{i+1}. \tag{1}$$

Define the target-fixed frame $\{\Gamma_{obj}\}$ where the origin is at the center of the target object, and X_{obj}-, Y_{obj}- and Z_{obj}-axes are parallel to x-, y- and z-axes of the inertial frame, respectively. Let $\mathbf{b}_i$ denote the projected vector of $\mathbf{d}_i$ onto the X_{obj}-Y_{obj} plane in the target-fixed frame, and define the following

---

[1]In the following, subscript '$n + 1$' is equivalent to '1'; i.e., the case that the i-th agent simply pursues the $(i + 1)$-th agent with modulo n is considered.

(a) Coordinate frames and notations
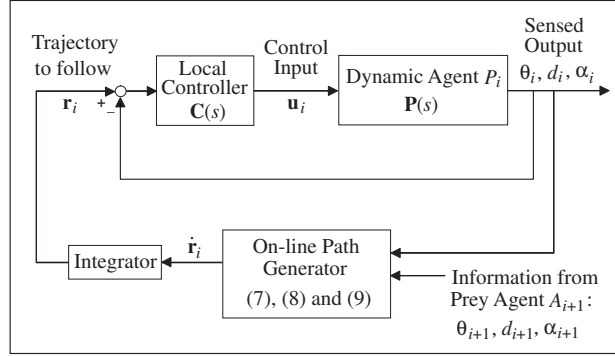
(b) Formation controller configuration

Figure 1: System description and formation controller configuration

scalars:

$$\theta_i = \angle(\mathbf{e}_x, \mathbf{b}_i), \quad \alpha_i = \angle(\mathbf{b}_i, \mathbf{d}_i), \quad d_i := |\mathbf{d}_i|, \tag{2}$$

where $\mathbf{e}_x$ denotes the unit vector in the X_{obj}-direction of $\{\Gamma_{obj}\}$, and $\angle(\mathbf{x}, \mathbf{y})$ denotes the counter-clockwise angle from the vector $\mathbf{x}$ to the vector $\mathbf{y}$. Then, $\mathbf{d}_i$ can be represented as $\mathbf{d}_i = [d_i \cos\theta_i \cos\alpha_i, d_i \sin\theta_i \cos\alpha_i, d_i \sin\alpha_i]^T$. Note that θ_{i+1} and $\delta\theta_i(:= \theta_{i+1} - \theta_i)$ can be calculated in a similar way based on (1), since $\mathbf{d}_{i+1} = \mathbf{d}_i - \mathbf{a}_i$ holds.

Suppose that all agents A_i $(i = 1, 2, \cdots, n)$ have common system dynamics described by a MIMO plant as follows:

$$\mathbf{y}_i(s) \quad := \left[\theta_i(s), d_i(s), \alpha_i(s)\right]^T = \mathbf{P}(s)\mathbf{u}_i(s) \tag{3}$$

where $\mathbf{y}_i(s)$ is the system output, $\mathbf{u}_i(s)$ is the control input, and $\mathbf{P}(s)$ is the

4

diagonal transfer matrix defined as

$$\mathbf{P}(s) := \operatorname{diag}(p_\theta(s), p_d(s), p_\alpha(s)).$$

In other words, we assume that θ-, d- and α-directional dynamics are independent of one another. Also assume that all agents are asymptotically stabilized by an identical local diagonal feedback controller $\mathbf{C}(s)$ defined as

$$\mathbf{C}(s) := \operatorname{diag}(c_\theta(s), c_d(s), c_\alpha(s))$$

as illustrated in Figure 1(b). Then, θ-, d- and α-directional closed-loop transfer functions of agent A_i are respectively described as

$$g_\theta(s) = \frac{p_\theta(s)c_\theta(s)}{1 + p_\theta(s)c_\theta(s)}, \tag{4}$$

$$g_d(s) = \frac{p_d(s)c_d(s)}{1 + p_d(s)c_d(s)}, \tag{5}$$

$$g_\alpha(s) = \frac{p_\alpha(s)c_\alpha(s)}{1 + p_\alpha(s)c_\alpha(s)}. \tag{6}$$

It is assumed that the above transfer functions satisfy the following conditions:

Assumption 1 *All the closed-loop transfer functions $g_\theta(s)$, $g_d(s)$ and $g_\alpha(s)$ are proper, stable, and have no zero at the origin of the complex plane.*

Now, we consider how to form a geometric pattern for the target-enclosing operation by n dynamic agents. The detailed control objectives are stated as follows:

($A1$) n agents enclose the target object at uniformly spaced angle and maintain this angle,

($A2$) Each agent approaches to the target object and finally keeps the distance D,

($A3$) The angle α_i which corresponds to the altitude of each agent converges to the desired one Φ,

where D and Φ are given by the designer[2].

In the next section, the distributed pursuit formation control scheme [8] is briefly presented. We then illustrate that the scheme cannot achieve the control objectives ($A1$)-($A3$) when it is applied to the case where each agent has a dynamics. Next, it is presented how a large-scale linear system description with a generalized frequency variable can be derived from our homogeneous multi-agent dynamical system.

---

[2]Note that for the sake of clarity and page limitation, this paper only considers the equal convergence positions for all dynamic agents; i.e., $D_1 = D_2 = \cdots = D_n = D$ and $\Phi_1 = \Phi_2 = \cdots = \Phi_n = \Phi$, while the distinct ones for each agent can be assigned.

3 Distributed formation control system

It is important from the practical viewpoint to achieve the desired global behavior through a relatively simple control law using only local information. As one of the feasible methods for realizing the required geometric formation $(A1)$-$(A3)$ mentioned in Section 2, we first present a design method of distributed on-line path generator motivated by a cyclic pursuit strategy [8]. Note that the parameters of this path generator should satisfy some conditions to guarantee the global convergence property, which is described in Sections 4 and 5 in detail.

3.1 Design of a distributed on-line path generator

It is assumed that n agents with dynamics are randomly dispersed in 3D space at the initial time instant as depicted in Figure 1(a), where $0 < |\delta\theta_i| < 2\pi$ for $i = 1, 2, \cdots, n$, and $\sum_{i=1}^{n} \delta\theta_i = 2\pi$. Then, the distributed on-line path planning scheme for the ith agent A_i is described as

$$\dot{r}_i^\theta(t) = k_\theta \delta\theta_i(t), \tag{7}$$
$$\dot{r}_i^d(t) = k_d(D - d_i(t)), \tag{8}$$
$$\dot{r}_i^\alpha(t) = k_\alpha(\Phi - \alpha_i(t)), \tag{9}$$

where k_θ, k_d, and k_α (> 0) are design parameters, and $\delta\theta_i(t)$ is defined by

$$\begin{cases} \delta\theta_i(t) := \theta_{i+1}(t) - \theta_i(t), & i = 1, 2, \cdots, n-1 \\ \delta\theta_n(t) := \theta_1(t) - \theta_n(t) + 2\pi, & i = n. \end{cases}$$

It is important to note that the gains k_θ, k_d, and k_α should satisfy some conditions to guarantee the achievement of the desired global formation $(A1)$-$(A3)$, which will be explained later in detail. Then, the reference position $\mathbf{r}_i(t) = [r_i^\theta(t), r_i^d(t), r_i^\alpha(t)]^T$ for the ith agent A_i shown in Figure 1(b) is designed by (7), (8) and (9).

It should be emphasized that, in the proposed path planning method, each agent individually decides its reference position based on the local information on only one other agent and the target object, which is probably a minimum of information exchanges between agents. Further, it has additional distinctive features as follows: each agent individually obtains the required information using the sensor systems implemented on its body, which means that no centralized communication mechanism between agents is introduced. Also, it is a memoryless controller in the sense that each agent determines the next behavior based only on the current position of its prey, independently of the past behavior of its prey. Thus, it is an easily implementable method from the engineering viewpoint [8].
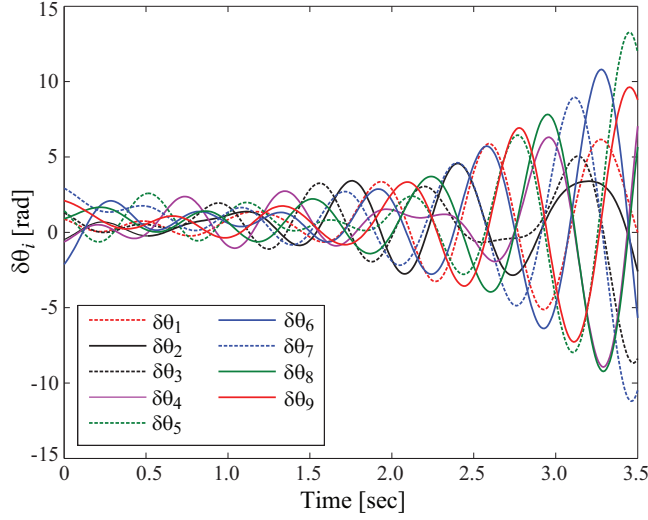
Figure 2: Plot showing the divergence of the relative angles $\delta\theta_i$[rad] ($i = 1, 2, \cdots, 9$)

Now, the control objectives $(A1)$-$(A3)$ in Section 2 can be formulated algebraically as follows:

$(A1')$ $\delta\theta_i(t) \to 2\pi/n$[rad] as $t \to \infty$,

$(A2')$ $d_i(t) \to D$ as $t \to \infty$,

$(A3')$ $\alpha_i(t) \to \Phi$[rad] as $t \to \infty$,

for $i = 1, 2, \cdots, n$. It has been proved in [8] that path planning schemes (7)-(9) can achieve the above control objectives $(A1')$-$(A3')$ under the assumption that each agent in the group is supposed to be a point mass. However, when agents' dynamics such as (4)-(6) are considered explicitly, the achievement of the stable global formation $(A1')$-$(A3')$ may not be guaranteed only by the condition that k_θ, k_d and k_α in (7)-(9) are positive real numbers. The following example illustrates this fact clearly.

Example 1 *We here investigate only the θ-directional behaviors of $n = 9$ agents for the sake of clarity. The initial values of $\theta_i(t)$[rad] are set as $\theta_1 = 0.198$, $\theta_2 = 1.269$, $\theta_3 = 0.050$, $\theta_4 = 1.491$, $\theta_5 = 1.175$, $\theta_6 = 0.189$, $\theta_7 = 2.045$, $\theta_8 = 0.793$, $\theta_9 = 1.712$. Assume that the common θ-directional agent dynamics is given by $p_\theta(s) = 1/s(s-1)$ which is stabilized by a PD controller $c_\theta(s) = 12(1 + 0.25s)$. The reference position $r_i^\theta(t)$ for agent A_i is designed based on (7) with $k_\theta = 0.4$. The time responses of $\delta\theta_i(t)$ $(i = 1, 2, \cdots, 9)$ are illustrated in Figure 2, which clearly shows that no $\delta\theta_i$ converges to $2\pi/9$[rad]. It demonstrates the formation instability.*

One can see from the above observation that three gains k_θ, k_d and k_α should be set carefully, in order to achieve the global formation $(A1')$-$(A3')$.

Hence, in the following subsection, it is presented in advance of deriving these conditions how a large-scale linear system description with a generalized frequency variable can be formulated for the homogeneous multi-agent dynamic system in Figures 1(a)-1(b).

3.2 Large-scale linear system description with a generalized frequency variable

In order to analyze the formation stability of multi-agent dynamical systems considered in Section 3.1, we rewrite (7) in the following vector form:

$$
\begin{aligned}
\dot{\mathbf{r}}^\theta(t) &= A_\theta \boldsymbol{\theta}(t) + B_\theta, \\
A_\theta &:= \text{circ}(-k_\theta,\ k_\theta,\ 0,\ 0, \cdots,\ 0) \in \mathbb{R}^{n \times n}, \\
B_\theta &:= [0,\ 0, \cdots,\ 0,\ 2k_\theta \pi]^T \in \mathbb{R}^n,
\end{aligned}
\tag{10}
$$

where $\boldsymbol{\theta} := [\theta_1, \theta_2, \cdots, \theta_n]^T \in \mathbb{R}^n$, $\mathbf{r}^\theta := [r_1^\theta, r_2^\theta, \cdots, r_n^\theta]^T \in \mathbb{R}^n$ and 'circ' denotes the circulant matrix. Thus, the overall $\boldsymbol{\theta}$-directional control scheme can be depicted as in Figure 3, where

$$
h_\theta(s) := g_\theta(s) \cdot \frac{1}{s}
\tag{11}
$$

is strictly proper from Assumption 1. Here, it is important to note that the eigenvalues $\{\lambda_i\}_{i=1}^n$ of A_θ can be written in the following complex form, since it is a circulant matrix:

$$
\lambda_i = k_\theta \left[\cos\left(\frac{2\pi(i-1)}{n} \right) - 1 \right] + jk_\theta \sin\left(\frac{2\pi(i-1)}{n} \right)
\tag{12}
$$

where $j := \sqrt{-1}$. Since $k_\theta > 0$, A_θ has exactly one zero eigenvalue, λ_1, while the remaining $n - 1$ eigenvalues λ_i, $i = 2, 3, \cdots, n$, lie strictly in the left-half complex plane. In the same manner, (8) and (9) can be rewritten, respectively, as

$$
\dot{\mathbf{r}}^d(t) = A_d \boldsymbol{d}(t) + B_d,
\tag{13}
$$

$$
\dot{\mathbf{r}}^\alpha(t) = A_\alpha \boldsymbol{\alpha}(t) + B_\alpha,
\tag{14}
$$

with $\boldsymbol{d} := [d_1, d_2, \cdots, d_n]^T \in \mathbb{R}^n$, $\boldsymbol{\alpha} := [\alpha_1, \alpha_2, \cdots, \alpha_n]^T \in \mathbb{R}^n$, $A_d := -\text{diag}(k_d, k_d, \cdots, k_d) \in \mathbb{R}^{n \times n}$, $B_d := (k_d D)\mathbf{1}_n \in \mathbb{R}^n$, $A_\alpha := -\text{diag}(k_\alpha, k_\alpha, \cdots, k_\alpha) \in \mathbb{R}^{n \times n}$, $B_\alpha := (k_\alpha \Phi)\mathbf{1}_n \in \mathbb{R}^n$ where $\mathbf{1}_n := [1, 1, \cdots, 1]^T \in \mathbb{R}^n$. The block diagrams of the $\boldsymbol{d}$- and $\boldsymbol{\alpha}$-directional formation controlled systems have the same form with that in Figure 3.

In Figure 3, the transfer function $\mathcal{H}_\theta(s)$ from the input "c" to $\boldsymbol{\theta}$ is obtained as

$$
\mathcal{H}_\theta(s) = \left(\frac{1}{h_\theta(s)} I_n - A_\theta \right)^{-1} B_\theta.
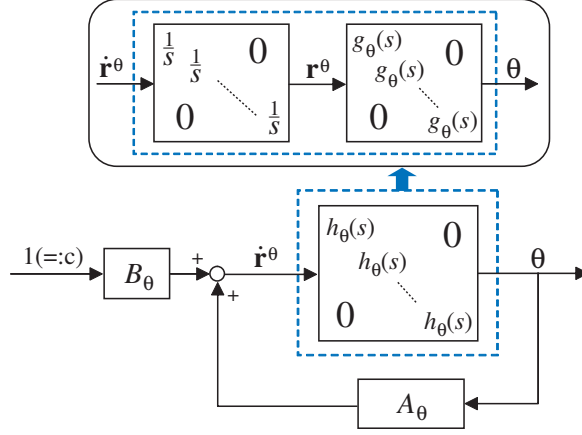\tag{15}
$$

Figure 3: Block diagram of the $\boldsymbol{\theta}$-directional formation controlled system: $\mathcal{H}_\theta(s)$

By considering the transfer function with a standard form

$$L_\theta(s) = (sI_n - A_\theta)^{-1}B_\theta, \tag{16}$$

it follows from (15) that

$$\mathcal{H}_\theta(s) = L_\theta(\phi_\theta(s)), \quad \phi_\theta(s) := 1/h_\theta(s). \tag{17}$$

Note that $\phi_\theta(0) = 0$ from Assumption 1 and (11). The variable 's' in (16) characterizes the frequency properties of the transfer function $L_\theta(s)$ and $\mathcal{H}_\theta(s)$ is generated by just replacing 's' by '$\phi_\theta(s)$' in $L_\theta(s)$. Hence, we say that the transformed transfer function $\mathcal{H}_\theta(s) = L_\theta(\phi_\theta(s))$ of $L_\theta(s)$ has a generalized frequency variable $\phi_\theta(s)$ (see [3] for details). Similarly, the $\boldsymbol{d}$- and $\boldsymbol{\alpha}$-directional transfer functions $\mathcal{H}_d(s)$ and $\mathcal{H}_\alpha(s)$ can be derived as:

$$\mathcal{H}_d(s) = L_d(\phi_d(s)), \ \phi_d(s) := 1/h_d(s) = s/g_d(s), \tag{18}$$
$$\mathcal{H}_\alpha(s) = L_\alpha(\phi_\alpha(s)), \ \phi_\alpha(s) := 1/h_\alpha(s) = s/g_\alpha(s). \tag{19}$$

It is important to note that as the growth in agent numbers, the size of the matrix in $\mathcal{H}_\theta(s)$ becomes very large, which is also the case for $\mathcal{H}_d(s)$ and $\mathcal{H}_\alpha(s)$. This fact results in a considerable increase of computational complexity in formation stability analysis. Therefore, in the following sections, we first develop a very simple Lyapunov stability analysis method which is independent of a number of dynamic agents. Then, some important results on the agents' convergence property in distributed formation control are presented.

4 Lyapunov stability analysis scheme for distributed formation control

The notations which will be used throughout this paper are first introduced: the domains Ω_θ, Ω_θ^c, Ω_d, Ω_d^c, Ω_α and Ω_α^c in the complex plane are defined as

$$\Omega_\theta := \phi_\theta(\mathbb{C}_+), \quad \Omega_\theta^c := \mathbb{C} \backslash \Omega_\theta, \qquad (20)$$

$$\Omega_d := \phi_d(\mathbb{C}_+), \quad \Omega_d^c := \mathbb{C} \backslash \Omega_d, \qquad (21)$$

$$\Omega_\alpha := \phi_\alpha(\mathbb{C}_+), \quad \Omega_\alpha^c := \mathbb{C} \backslash \Omega_\alpha, \qquad (22)$$

where $\mathbb{C}$ denotes the set of complex numbers, and $\mathbb{C}_+ = \{s \in \mathbb{C} : \text{Re}[s] \geq 0\}$. Since $\Omega_\bullet = \{\lambda \in \mathbb{C} : \exists s \in \mathbb{C}_+ \text{ such that } \phi_\bullet(s) = \lambda\}$ ($\bullet = \theta, d, \alpha$), it follows that $\Omega_\bullet^c$ can be alternatively expressed as $\Omega_\bullet^c = \{\lambda \in \mathbb{C} : \forall s \in \mathbb{C}_+, \ \phi_\bullet(s) \neq \lambda\}$ ($\bullet = \theta, d, \alpha$).

Before deriving a stability condition for the system $\mathcal{H}_\theta(s)$ in (17), we first describe a key result on stability analysis of large-scale linear systems with a generalized frequency variable developed by [3]. In their paper, the following *asymptotic* stability criterion is presented: all poles of $\mathcal{H}_\theta(s)$ are located in the left-half complex plane, if and only if all eigenvalues of A_θ in (10) belong to the domain Ω_θ^c. However, the matrix A_θ denoting information exchange structure among multiple dynamic agents has one zero eigenvalue ($\lambda_1 = 0$) as shown in (12), and $\phi_\theta(s)$ in (17) satisfies $\phi_\theta(0) = 0$. It means that for any positive value of k_θ, this zero eigenvalue is always located on the boundary of Ω_θ, and thus cannot belong to the domain $\Omega_\theta^{c \, 3}$. On the other hand, A_d in (13) and A_α in (14) have n multiple eigenvalues at $(-k_d + j0)$ and $(-k_\alpha + j0)$, respectively, and hence their stability analysis can be performed using the above-mentioned criterion in [3]. Therefore, in the following, a novel Lyapunov stability analysis scheme for the multi-agent dynamical systems such as $\mathcal{H}_\theta(s)$ where A_θ has a zero eigenvalue is developed.

The following proposition describes a range of pole locations of $\mathcal{H}_\theta(s)$ in relation to the eigenvalue distribution of A_θ in (10) and the region which $\phi_\theta(s)$ in (17) maps the right-half complex plane to.

Proposition 1 *Suppose that $g_\theta(s)$ in (4) satisfies Assumption 1. Then, the following statements are equivalent:*

(i) One of the eigenvalues of A_θ is at the origin of the complex plane, and the rest belong to the domain Ω_θ^c,

(ii) One of the poles of $\mathcal{H}_\theta(s)$ is at the origin of the complex plane, and the rest belong to the open left-half complex plane.

---

[3]The same problem may happen in consensus problem of multi-agent network systems; e.g., graph Laplacian matrix which is usually introduced to describe the information flow among agents in consensus problems has a zero eigenvalue.
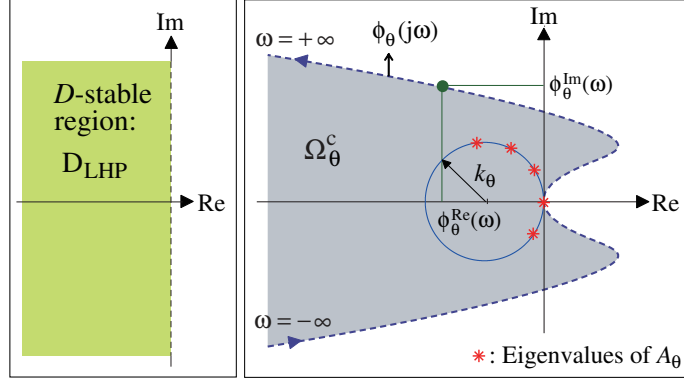
Figure 4: The eigenvalues λ_i $(i = 1, 2, \cdots, n)$ of A_θ and the domain Ω_θ^c

Proof Let n eigenvalues of A_θ be denoted by $\{\lambda_1 = 0, \lambda_2, \lambda_3, \cdots, \lambda_n\}$. The poles of $\mathcal{H}_\theta(s)$ are identical, including multiplicity, to the roots of $|\phi_\theta(s)I_n - A_\theta| = 0$ (see Appendix A for details.). It follows from the factorization of $|\phi_\theta(s)I_n - A_\theta| = 0$ that

$$\phi_\theta(s)(\phi_\theta(s) - \lambda_2)(\phi_\theta(s) - \lambda_3) \cdots (\phi_\theta(s) - \lambda_n) = 0. \tag{23}$$

Then, the necessary and sufficient condition for the existence of all roots of

$$(\phi_\theta(s) - \lambda_2)(\phi_\theta(s) - \lambda_3) \cdots (\phi_\theta(s) - \lambda_n) = 0 \tag{24}$$

in the open left-half complex plane is that $\{\lambda_2, \lambda_3, \cdots, \lambda_n\} \in \Omega_\theta^c$. Further, it follows from Assumption 1 and the definition of $\phi_\theta(s)$ that one root of $\phi_\theta(s) = 0$ is $s = 0$, and the rest are located in the open left-half complex plane. Therefore, we can see from the above observations that one of the poles of $\mathcal{H}_\theta(s)$ is at the origin of the complex plane, and the rest are located in the open left-half complex plane (see Figure 4). $\square$

The above proposition means that the Lyapunov stability of $\mathcal{H}_\theta(s)$ can be judged diagrammatically by just looking at the locations of eigenvalues of A_θ which is derived from path generator in relation to a domain Ω_θ^c determined by using $\phi_\theta(s)$. More precisely, we can see from Proposition 1 that $\mathcal{H}_\theta(s)$ has one pole at the origin and $n-1$ poles in the left-half complex plane (i.e., $\mathcal{H}_\theta(s)$ is Lyapunov stable), if all eigenvalues of A_θ except one zero eigenvalue belong to the domain Ω_θ^c.

5 Global tracking property in distributed pursuit formation control

This section shows that the required geometric formation $(A1')$-$(A3')$ mentioned in Section 3.1 is realized, if both the following two conditions are
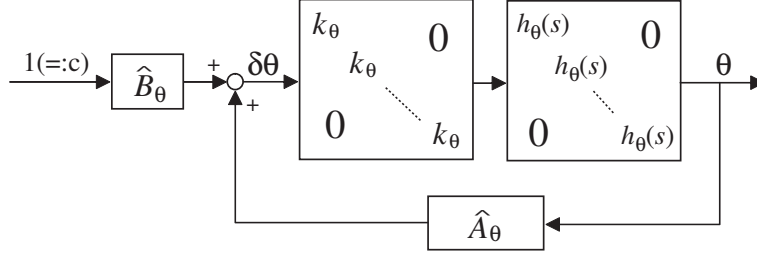
11

Figure 5: Equivalent form of the block diagram in Figure 3

satisfied:

(I) $\mathcal{H}_\theta(s)$ is Lyapunov stable,

(II) $\mathcal{H}_d(s)$ and $\mathcal{H}_\alpha(s)$ are asymptotic stable.

We first show that the control objective $(A1')$ can be achieved in case that eigenvalue distributions of A_θ in (10) satisfy the conditions in Proposition 1, and thus Lyapunov stability of $\mathcal{H}_\theta(s)$ in (15) is guaranteed. The following theorem describes a global convergence property of $\delta\theta_i(t)$ $(i = 1, 2, \cdots, n)$ when all nonzero eigenvalues $\{\lambda_i\}_{i=2}^n$ of A_θ belong to the domain Ω_θ^c.

Theorem 1 *Consider the system consisting of n agents with angle dynamics $g_\theta(s)$ which are randomly dispersed in 3D space at the initial time instant as shown in Figure 1(a), where $0 < |\delta\theta_i(0)| < 2\pi$ $(i = 1, 2, \cdots, n)$ and $\sum_{i=1}^n \delta\theta_i(0) = 2\pi$. It is assumed that agent's θ-directional transfer function $g_\theta(s)$ in (4) satisfies Assumption 1. Then, if all eigenvalues of A_θ except one zero eigenvalue belong to the domain Ω_θ^c, the following convergence property of $\delta\theta_i(t)$ is guaranteed:*

$$\lim_{t\to\infty} \delta\theta_i(t) \to 2\pi/n[\text{rad}], \quad i = 1, 2, \cdots, n. \tag{25}$$

Proof In order to examine the convergence value of $\delta\theta_i(t)$ for $i = 1, 2, \cdots, n$, we first consider how to obtain a transfer function from the input "c" in Figure 3 to $\delta\boldsymbol{\theta}$. Note that the block diagram in Figure 5 is equivalent to the one in Figure 3 for $\mathcal{H}_\theta(s)$, where $\hat{A}_\theta := \text{circ}(-1, 1, \cdots, 0) \in \mathbb{R}^{n\times n}$ and $\hat{B}_\theta := [0, 0, \cdots, 2\pi]^T \in \mathbb{R}^n$. Then, from Figure 5, the closed-loop transfer function $\mathcal{W}(s)$ from "c" to $\delta\boldsymbol{\theta}$ is obtained as

$$\mathcal{W}(s) = \left(I_n - k_\theta h_\theta(s)\hat{A}_\theta\right)^{-1} \hat{B}_\theta. \tag{26}$$

Since $\hat{A}_\theta$ is a circulant matrix, this matrix is diagonalizable by the following discrete Fourier transform matrix $F \in \mathbb{C}^{n \times n}$ [1]:

$$F := \frac{1}{\sqrt{n}} \begin{bmatrix} 1 & 1 & 1 & \cdots & 1 \\ 1 & \omega & \omega^2 & \cdots & \omega^{n-1} \\ 1 & \omega^2 & \omega^4 & \cdots & \omega^{2(n-1)} \\ \vdots & \vdots & \vdots & \ddots & \vdots \\ 1 & \omega^{n-1} & \omega^{2(n-1)} & \cdots & \omega^{(n-1)(n-1)} \end{bmatrix} \tag{27}$$

where $\omega := e^{-j2\pi/n}$. Note that $F^{-1} = F^*$ holds where F^* is the conjugate transpose of F. Thus, we have

$$\begin{aligned} \mathcal{W}(s) &= F \left(I_n - k_\theta h_\theta(s) F^{-1} \hat{A}_\theta F \right)^{-1} \left(F^{-1} \hat{B}_0 \right) \\ &= F \left(I_n - k_\theta h_\theta(s) \Lambda \right)^{-1} \left(F^{-1} \hat{B}_\theta \right) \end{aligned} \tag{28}$$

where $\Lambda = \mathrm{diag}(\Delta_1, \Delta_2, \cdots, \Delta_n)$ with

$$\Delta_i := \left[\cos\left(\frac{2\pi(i-1)}{n} \right) - 1 \right] + j \sin\left(\frac{2\pi(i-1)}{n} \right).$$

Then, (28) can be rewritten as

$$\mathcal{W}(s) = F\Gamma(s) \left(F^{-1} \hat{B}_\theta \right) \tag{29}$$

where $\Gamma(s) := \mathrm{diag}(1, s/(s - k_\theta g_\theta(s)\Delta_2), \cdots, s/(s - k_\theta g_\theta(s)\Delta_n)) \in \mathbb{R}^{n \times n}$. It follows from $g_\theta(0) \neq 0$ (see Assumption 1) and the final-value theorem of Laplace transform theory that the final value of the step response of $\mathcal{W}(s)$ is given by

$$\begin{aligned} \lim_{s \to 0} \mathcal{W}(s) &= \lim_{s \to 0} F\Gamma(s)F^{-1}\hat{B}_\theta \\ &= \left[\frac{2\pi}{n}, \frac{2\pi}{n}, \cdots, \frac{2\pi}{n} \right]^T \in \mathbb{R}^n, \end{aligned} \tag{30}$$

which verifies (25). $\qquad\square$

The above theorem means that if the Lyapunov stability condition given in Proposition 1 holds, the control objective $(A1')$ is achieved.

Remember that the d- and α-directional asymptotic stabilities can be analyzed by using the scheme given in Hara et al. [3]: i.e., the necessary and sufficient asymptotic stability condition for $\mathcal{H}_d(s)$ ($\mathcal{H}_\alpha(s)$) is that all eigenvalues of A_d (A_α) belong to the domain Ω_d^c (Ω_α^c). Then, the following theorem for the convergence values of $d_i(t)$ and $\alpha_i(t)$ ($i = 1, 2, \cdots, n$) is derived:
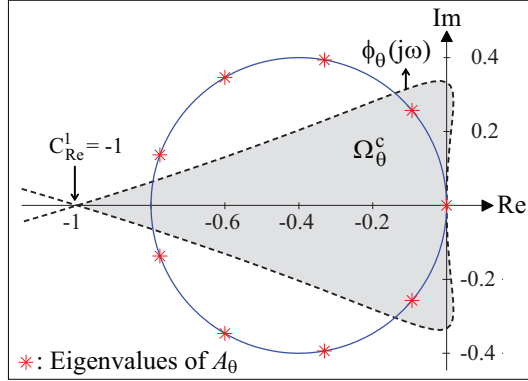
Figure 6: The domain Ω_θ^c and the eigenvalues of A_θ

Theorem 2 *Consider the system consisting of n agents with $g_\theta(s)$ angle dynamics which are randomly dispersed in 3D space at the initial time instant as shown in Figure 1(a). It is assumed that agent's transfer functions $g_d(s)$ in (5) and $g_\alpha(s)$ in (6) satisfy Assumption 1, and D in (A2′) and Φ in (A3′) are given in advance. Then, if all eigenvalues of A_d and A_α, respectively, belong to the domains Ω_d^c and Ω_α^c, the following convergence properties of $d_i(t)$ and $\alpha_i(t)$ are guaranteed: for $i = 1, 2, \cdots, n$,*

$$\lim_{t\to\infty} d_i(t) \to D, \tag{31}$$

$$\lim_{t\to\infty} \alpha_i(t) \to \Phi. \tag{32}$$

Its proof is self-evident and hence is omitted. In Theorems 1 and 2, the conditions for achieving the designated target-enclosing formation $(A1')$-$(A3')$ by multiple dynamic agents are derived, where we use the relations between the eigenvalue locations of A_θ, A_d, A_α and the domains Ω_θ^c, Ω_d^c, Ω_α^c. These imply how to determine k_θ, k_d and k_α of (7)-(9) in order to guarantee that all agents assemble into the desired formation around the target object in 3D space. For example, consider the multi-agent dynamical system given in Example 1, where k_θ was set as $k_\theta = 0.4$. In that case, the pole locations of $L_\theta(s)$ and the domain Ω_θ^c are as illustrated in Figure 6. It verifies that two poles of $L_\theta(s)$ do not belong to Ω_θ^c. Consequently, one reaches the conclusion that $(A1')$ cannot be achieved, which is evident from Figure 2. From the above observation and the details mentioned in Section 4, the following conclusions can be made:

(I') if $\mathcal{H}_\theta(s)$ is Lyapunov stable, then the control objective $(A1')$ for target-enclosing formation is achieved,

(II') if $\mathcal{H}_d(s)$ and $\mathcal{H}_\alpha(s)$ are asymptotic stable, then the control objectives

14

$(A2')$ and $(A3')$ are achieved.

In the following sections, we develop an explicit stabilization strategy of multi-agent dynamical systems for cyclic pursuit behavior based on the above results.

6   Stabilization strategy in distributed pursuit formation control

Although Proposition 1 in Section 4 and Theorems 1-2 in Section 5 provide a considerably simple formation stability analysis method and the resulting global tracking property, no explicit information about the transient performance of the designed formation control laws is obtained. For example, see the dotted line in Figure 10 which corresponds to the connectivity gain $k_\theta = 0.2374$. In this case, the used k_θ satisfies the given stability condition, but it produces an unsatisfactory convergence behavior of $\delta\theta_i(t)$ $(i = 1, 2, \cdots, 8)$. Note that, for the sake of page limitation, we mainly consider hereafter the θ-directional control scheme.

In order to overcome the above problem, we consider the Lypunov $\mathcal{D}$-stability problem: i.e., placing the poles of linear time-invariant system $\mathcal{H}_\theta(s)$ except one zero pole at a predesignated region of the complex plane, which is formulated as

---

Problem A: (Lypunov $\mathcal{D}$-stability problem) Derive a Lypunov stability criterion for global pursuit formation that enables us to judge whether all nonzero poles of $\mathcal{H}_\theta(s)$ in (15) belong to the $\mathcal{D}$-stable region, D_φ in Figure 7(a), which is characterized as

$$D_\varphi := \{s := \kappa e^{j\hat{\varphi}} \in \mathbb{C} : \varphi < \hat{\varphi} < 2\pi - \varphi, \ \forall\kappa > 0\} \qquad (33)$$

where φ $(\pi/2 \leq \varphi < \pi)$ is given a priori.

To this aim, we first define the domains Ω_φ and Ω_φ^c in the complex plane, which are the generalization of the definitions of domains Ω_θ and Ω_θ^c in (20):

$$\Omega_\varphi := \phi_\theta(\mathbb{C}_\varphi), \quad \Omega_\varphi^c := \mathbb{C}\backslash\Omega_\varphi, \qquad (34)$$

where $\mathbb{C}_\varphi = \{s := \kappa e^{j\vartheta} \in \mathbb{C} : -\varphi \leq \vartheta \leq \varphi, \ \forall\kappa \geq 0\}$. Note that the domain Ω_φ^c does not include the origin of the complex plane. Then, the key result which provides the Lyapunov $\mathcal{D}$-stability criterion for $\mathcal{H}_\theta(s)$ mentioned in "Problem A" is obtained as follows:
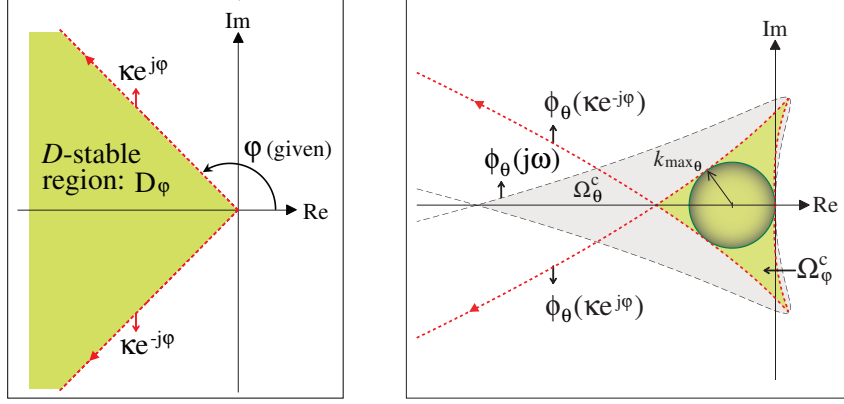
(a) The $\mathcal{D}$-stable region for locations of all non-zero poles of $\mathcal{H}_\theta(s)$

(b) The domain Ω_φ^c and the image of $\phi_\theta(\kappa e^{\pm j\varphi})$ where $\kappa \geq 0$ and $0 \leq \varphi \leq \pi$

Figure 7: The image of $\phi_\theta(\kappa e^{\pm j\varphi})$ and the corresponding domain Ω_φ^c

---

Proposition 2 *Suppose that $g_\theta(s)$ in (4) satisfies Assumption 1. Then, the following statements are equivalent:*

(i) One of the eigenvalues of A_θ is at the origin of the complex plane, and the rest belong to the domain Ω_φ^c,

(ii) One of the poles of $\mathcal{H}_\theta(s)$ is at the origin of the complex plane, and the rest belong to the $\mathcal{D}$-stable region D_φ of the complex plane illustrated in Figure 7(a).

It is proved in the same manner that we proved Proposition 1, and thus is omitted here. This proposition means that the Lypunov $\mathcal{D}$-stability of $\mathcal{H}_\theta(s)$ in "Problem A" can be judged diagrammatically by just looking at the locations of eigenvalues of A_θ depending on k_θ in relation to a domain Ω_φ^c which is determined by using $h_\theta(s)$. More precisely, we can see from Proposition 2 that $\mathcal{H}_\theta(s)$ has one pole at the origin and $n-1$ poles in the predesignated region D_φ (i.e., $\mathcal{H}_\theta(s)$ is Lyapunov $\mathcal{D}$-stable), if all eigenvalues of A_θ except one zero eigenvalue belong to the domain Ω_θ^φ. Note that the global tracking property given in Theorem 1 is also guaranteed, when $\mathcal{H}_\theta(s)$ is Lypunov $\mathcal{D}$-stable. Its distinctive features will be illustrated in Example 2 of the following subsection.

6.1 Pursuit formation stabilization scheme

In Proposition 2, we obtained a considerably simple diagrammatic Lyapunov $\mathcal{D}$-stability analysis method. On the other hand, it may be required to

find a maximum permissible limit of a connectivity gain k_θ satisfying the requirement presented in "Problem A" of the previous section. Therefore, we consider the following Lyapunov $\mathcal{D}$-stabilization problem in this section:

> **Problem S1**: Find the upper bound $k_{\max_\theta}$ of a connectivity gain k_θ in (10) guaranteeing that all nonzero poles of $\mathcal{H}_\theta(s)$ in (15) are placed in the predesignated $\mathcal{D}$-stable region D_φ defined in (33) and illustrated in Figure 7(a).

It is assumed hereafter in developing the Lyapunov $\mathcal{D}$-stabilization scheme for Problem S1 that the following condition is satisfied:

Assumption 2 *A connectivity gain $k_\theta (> 0)$ where $(-k_\theta + j0) \in \Omega_\varphi^c$ guarantees that the line segment between $(-k_\theta + j0)$ and the origin in the complex plane lies in Ω_φ^c.*

Then, from Proposition 2 and Figures 4 and 7, the condition, which guarantees all nonzero eigenvalues of A_θ with k_θ satisfying Assumption 2 belong to the domain Ω_φ^c characterized by $\kappa e^{\pm j\varphi}$ where φ is given by the designer, is derived as

$$(\phi_\varphi^{\mathrm{Re}}(\kappa) + k_\theta)^2 + (\phi_\varphi^{\mathrm{Im}}(\kappa))^2 > k_\theta^2, \quad \forall \kappa > 0, \tag{35}$$

where $\phi_\varphi^{\mathrm{Re}}(\kappa)$ and $\phi_\varphi^{\mathrm{Im}}(\kappa)$ are defined, respectively, as

$$\phi_\varphi^{\mathrm{Re}}(\kappa) := \mathrm{Re}[\phi_\theta(\kappa e^{j\varphi})], \quad \phi_\varphi^{\mathrm{Im}}(\kappa) := \mathrm{Im}[\phi_\theta(\kappa e^{j\varphi})].$$

Then, it follows from (35) that

$$(\phi_\varphi(\kappa e^{j\varphi}) + k_\theta)^*(\phi_\varphi(\kappa e^{j\varphi}) + k_\theta) > k_\theta^2, \tag{36}$$

which is equivalent to the the following inequality condition: for $\forall \kappa > 0$,

$$\left[\begin{array}{c} h_\theta(\kappa e^{j\varphi}) \\ 1 \end{array} \right]^* \Pi \left[\begin{array}{c} h_\theta(\kappa e^{j\varphi}) \\ 1 \end{array} \right] < 0, \quad \Pi := \left[\begin{array}{cc} 0 & -k_\theta \\ -k_\theta & -1 \end{array} \right]. \tag{37}$$

Therefore, the optimization problem to find the upper bound of a connectivity gain k_θ satisfying the requirement in "Problem S1" can be formulated as follows:

$$k_{\max_\theta} := \arg\max_{k_\theta, \kappa} k_\theta \quad \text{subject to (37) and } k_\theta > 0. \tag{38}$$

Hence, if one sets k_θ in (10) as $0 < k_\theta \le k_{\max_\theta}$, then all nonzero poles of $\mathcal{H}_\theta(s)$ in (15) are placed in the predesignated $\mathcal{D}$-stable region D_φ. However, since the constraint condition (37) should be checked for $\forall \kappa > 0$, the above optimization problem may not be easily solved.
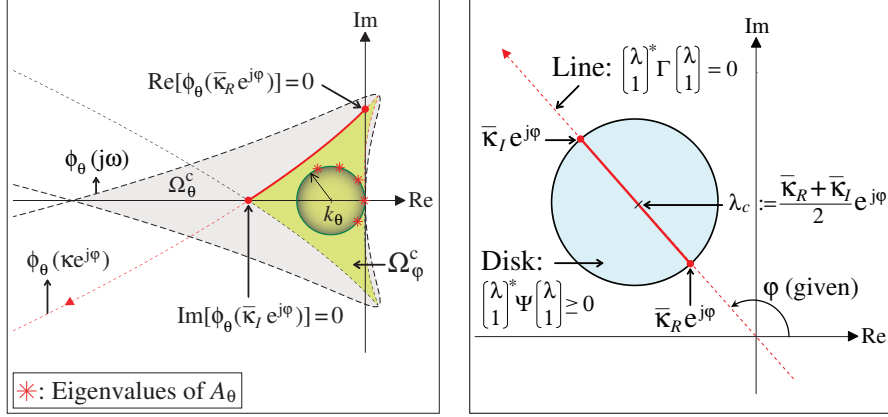
(a) The image of $\phi_\theta(\kappa e^{\pm j\varphi})$, $\forall \kappa \geq 0$, where φ(rad) is given a priori

(b) The set of complex numbers determined by $\boldsymbol{\Lambda}(\Gamma, \Psi)$ where Γ, Ψ are set as (41)

Figure 8: The image of $\phi_\theta(\kappa e^{j\varphi})$ and the set of complex numbers $\boldsymbol{\Lambda}(\Gamma, \Psi)$

In order to overcome the above difficulty, we then convert the inequality condition (37) to LMIs by using the GKYP lemma [4, 6]. Note that the LMIs are numerically tractable and can be solved efficiently. Now, we assume that the state-space realization of $h_\theta(s)$ is obtained as

$$h_\theta(s) = C_{h_\theta}(sI - A_{h_\theta})^{-1}B_{h_\theta} + D_{h_\theta}. \tag{39}$$

We then characterize the restricted range of κ to check the constraint condition (37) within a framework of the GKYP lemma. For example, if $\phi_\theta(s)(= 1/h_\theta(s))$ and φ are given, $\phi_\theta(\kappa e^{j\varphi})$ is readily obtained (see Figures 7 and 8). Then, $\bar{\kappa}_R$ and $\bar{\kappa}_I$ ($0 < \bar{\kappa}_R < \bar{\kappa}_I$) satisfying $\text{Re}[\phi_\theta(\bar{\kappa}_R e^{j\varphi})] = 0$ and $\text{Im}[\phi_\theta(\bar{\kappa}_I e^{j\varphi})] = 0$, respectively, are found via simple calculations (if exist). Now one can see from Figure 8(a) that it is sufficient to check the condition (37) in the range $\bar{\kappa}_R \leq \kappa \leq \bar{\kappa}_I$. In this case, the set of complex numbers $\boldsymbol{\Lambda}(\Gamma, \Psi)$ corresponding to the above-mentioned range of κ is defined as

$$\boldsymbol{\Lambda}(\Gamma, \Psi) := \left\{ \lambda \in \mathbb{C} : \begin{bmatrix} \lambda \\ 1 \end{bmatrix}^* \Gamma \begin{bmatrix} \lambda \\ 1 \end{bmatrix} = 0, \ \begin{bmatrix} \lambda \\ 1 \end{bmatrix}^* \Psi \begin{bmatrix} \lambda \\ 1 \end{bmatrix} \geq 0 \right\} \tag{40}$$

with

$$\Gamma := \begin{bmatrix} 0 & \tan\varphi - j \\ \tan\varphi + j & 0 \end{bmatrix}, \quad \Psi := \begin{bmatrix} -1 & \lambda_c \\ \bar{\lambda}_c & -\bar{\kappa}_R\bar{\kappa}_I \end{bmatrix}, \tag{41}$$

and $\lambda_c = \frac{\bar{\kappa}_R + \bar{\kappa}_I}{2}e^{j\varphi}$ (see Figure 8(b)). For details of choices of Γ and Ψ, refer to Iwasaki and Hara [6]. Therefore, under the setting (40) with (41), the

18
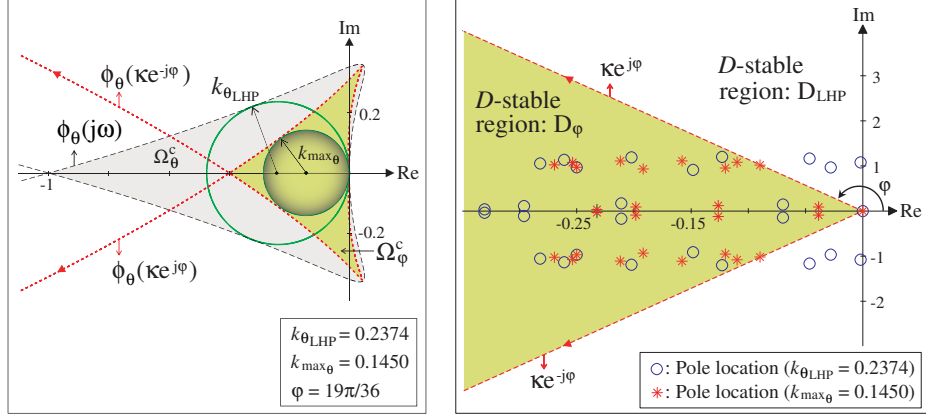
(a) The images of $\phi_\theta(j\omega)$, $\phi_\theta(\kappa e^{j\varphi})$ and the corresponding domains Ω_θ^c, Ω_φ^c

(b) The pole locations of $\mathcal{H}_\theta(s)$ with two different values of k_θ

Figure 9: Simulation results of Example 2

upper bound $k_{\max_\theta}$ of k_θ mentioned in "Problem S1" can easily be obtained by solving the following optimization problem subject to LMI constraint conditions:

Optimization problem for "Problem S1": For given $h_\theta(s) \sim (A_{h_\theta}, B_{h_\theta}, C_{h_\theta}, D_{h_\theta})$ and φ ($\pi/2 \leq \varphi < \pi$), solve

$$k_{\max_\theta} := \arg \max_{k_\theta, P \in \mathbf{H}_n, Q \in \mathbf{H}_n} k_\theta \qquad (42)$$

subject to $k_\theta > 0$ and

$$Q > 0, \; M^* Z M < 0, \qquad (43)$$

where $Z = \mathrm{diag}(\Gamma \otimes P + \Psi \otimes Q, \Pi)$ with Π in (37) and Γ and Ψ in (40)-(41), and

$$M := \begin{bmatrix} A_{h_\theta} & B_{h_\theta} \\ I & 0 \\ C_{h_\theta} & D_{h_\theta} \end{bmatrix}.$$

Note that the LMI constraint condition in (43), which is equivalent to (37), is derived based on the GKYP lemma [4, 6]. If one sets k_θ in (10) as $0 < k_\theta \leq k_{\max_\theta}$, then all nonzero poles of $\mathcal{H}_\theta(s)$ in (15) are placed in the predesignated $\mathcal{D}$-stable region (D_φ) in Figure 7(a). Its effectiveness is illustrated in the following example.
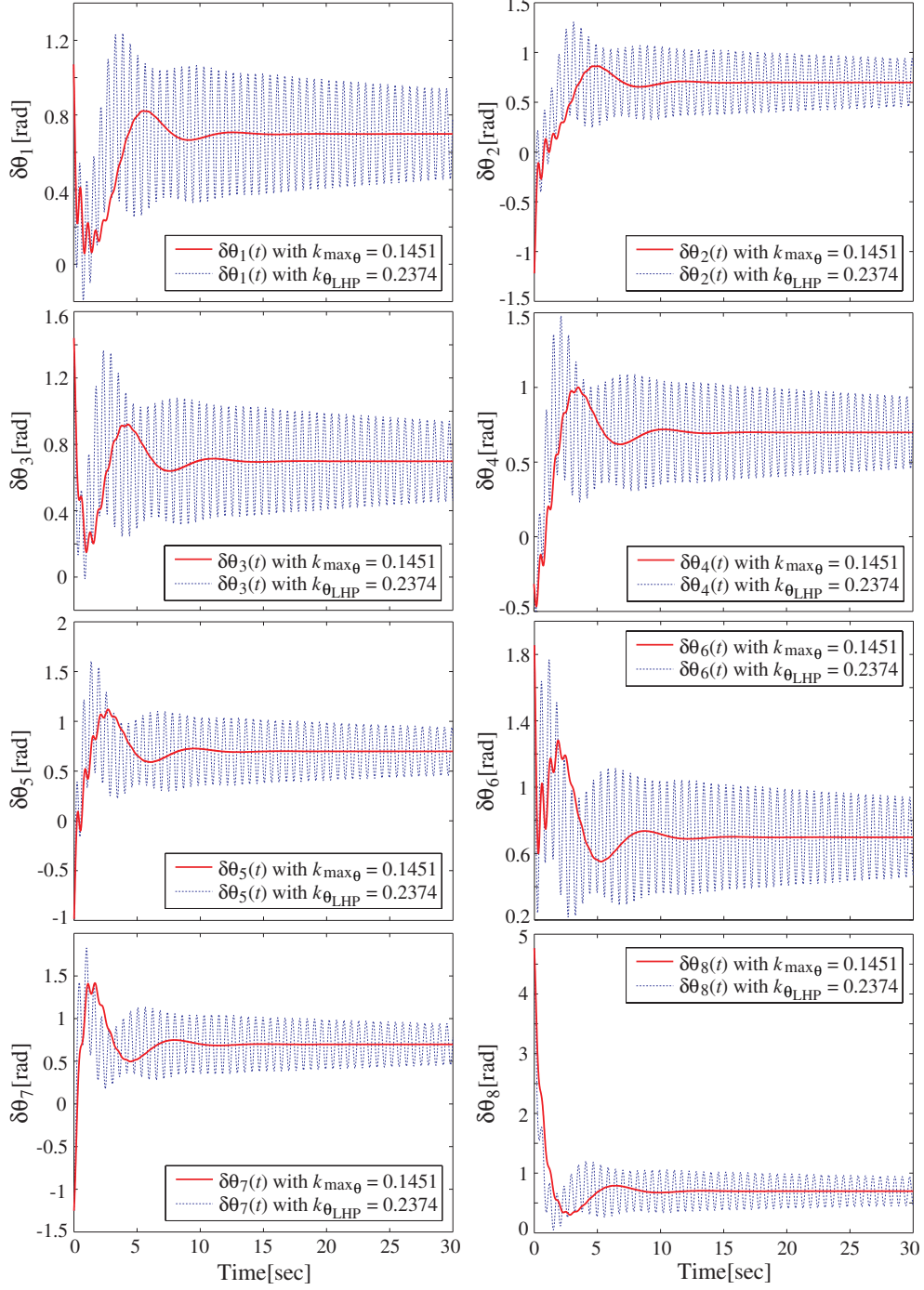
19

Figure 10: Time plots of $\delta\theta_i(t)$ $(i = 1, 2, \cdots, 8)$ for $k_\theta = 0.1451$ and 0.2374

Example 2 *Suppose that $n = 8$ agents have common dynamics $p_\theta(s) = 1/s(s-0.5)$ and its stabilizing PD controller is given as $c_\theta(s) = 1+s$. In this case, the images of $\phi_\theta(j\omega)$ and $\phi_\theta(\kappa e^{j\varphi})$ with $\varphi = 19\pi/36\,(rad)$ are illustrated in Figure 9(a). Here, $k_{\theta_{\mathrm{LHP}}} = 0.23742$ [5], which enables all nonzero poles of $\mathcal{H}_\theta(s)$ to be located in the $\mathcal{D}$-stable region, D_{LHP}, as shown in Figure 9(b). Under the above system setting, we have $\bar{\kappa}_R \approx 0.7490$ and $\bar{\kappa}_I \approx 1.1573$. Then, the above optimization (42) with Γ and Ψ in (41) is solved by using the LMI Control Toolbox in MATLAB, and we obtain $k_{\max_\theta} \approx 0.14505$. Then, all pole locations of $\mathcal{H}_\theta(s)$ with $k_{\theta_{\mathrm{LHP}}} = 0.2374$ and $k_{\max_\theta} = 0.1450$ are depicted in Figure 9(b). From these figures, it can easily be confirmed that if it is required for all the poles of $\mathcal{H}_\theta(s)$ in (15) to be assigned to a predesignated region (the $\mathcal{D}$-stable region denoted by D_φ in Figure 9(b)), the only thing one should do is to find $k_{\max_\theta}$ and then set k_θ as $0 < k_\theta \leq k_{\max_\theta}$. The above fact shows that it is an easily implementable pole assignment technique. The time responses of $\delta\theta_i(t)$ $(i = 1, 2, \cdots, 8)$ for $k_\theta = 0.1450$ and 0.2374 are illustrated in Figure 10, which clearly demonstrates an advantage of the considering $\mathcal{D}$-stability.*

In the following section, in order to show clearly the distinctiveness and effectiveness of the proposed stabilization technique, we derive an explicit LMI optimization problem for a class of multi-agent systems combined with a cyclic pursuit based path generator, where each agent is modeled as a class of second-order systems and is locally stabilized by the PID controller.

7 Pursuit formation stabilization: Maximization of connectivity gain for PID controller case

In this section, we introduce a class of multi-agent dynamical systems locally stabilized by PID controllers, and then present how to stabilize this pursuit formation controlled systems based on the result given in Section 6. In order to make our idea clear, we set $\varphi = \pi/2$ (i.e., $\mathcal{D}$-stable region is D_{LHP} in Figure 4), since the extension to the general case $\pi/2 < \varphi < \pi$ is trivial.

7.1 A class of multi-agent dynamical systems locally stabilized by PID controllers

Assume that the homogeneous θ-directional agent dynamics is given as

$$p_\theta(s) = \frac{\zeta}{s(s+\xi)} \tag{44}$$

where $\zeta > 0$. Then, the PID controller $c_\theta(s)$ such as

$$c_\theta(s) = k_p \left(1 + \frac{1}{t_i s} + t_d s \right), \tag{45}$$

where $k_p > 0$, $t_i > 0$ and $t_d > 0$, is introduced to stabilize (44). Hence, it follows from $p_\theta(s)$ and $c_\theta(s)$ that

$$g_\theta(s) = \frac{t_d t_i s^2 + t_i s + 1}{(t_i/\zeta k_p)s^3 + (\xi t_i/\zeta k_p + t_d t_i)s^2 + t_i s + 1}. \tag{46}$$

Let $\tilde{s} = t_i s$. Then, (46) can be modified as

$$g_\theta(\tilde{s}) = \frac{a\tilde{s}^2 + \tilde{s} + 1}{b\tilde{s}^3 + (a + c)\tilde{s}^2 + \tilde{s} + 1} \tag{47}$$

where $a := t_d/t_i (> 0)$, $b := 1/(\zeta k_p t_i^2)(> 0)$, $c := \xi/(\zeta k_p t_i)$. Therefore, without loss of generality, the following form of the generalized frequency variable $\phi_\theta(s)$ can be considered hereafter:

$$\phi_\theta(s) = \frac{1}{h_\theta(s)} = \frac{s}{g_\theta(s)} = \frac{bs^4 + (a + c)s^3 + s^2 + s}{as^2 + s + 1}. \tag{48}$$

Note that $g_\theta(s)$ is stable, if and only if $a + c > b$.

Next, we characterize the domains Ω_θ and Ω_θ^c defined as (20) in the complex plane. These regions are partitioned by the image of $\phi_\theta(j\omega)$ in (48) where $\omega \in \mathbb{R}$. Define $\phi_\theta^{\mathrm{Re}}(\omega) := \mathrm{Re}\,[\phi_\theta(j\omega)]$ and $\phi_\theta^{\mathrm{Im}}(\omega) := \mathrm{Im}\,[\phi_\theta(j\omega)]$ as follows:

$$\phi_\theta^{\mathrm{Re}}(\omega) = \frac{\omega^4(-ab\omega^2 + b - c)}{(1 - a\omega^2)^2 + \omega^2}, \tag{49}$$

$$\phi_\theta^{\mathrm{Im}}(\omega) = \frac{(a^2 + ac - b)\omega^5 + (1 - 2a - c)\omega^3 + \omega}{(1 - a\omega^2)^2 + \omega^2}. \tag{50}$$

Then, the image of $\phi_\theta(j\omega)$ yields six types of diagrams as shown in Figure 11 where $\mathbf{R}_+$ denotes the positive real number. If $b > c$ which is equivalent to $\xi < 1/t_i$, the image of $\phi_\theta(j\omega)$ corresponds to Case B-1, B-2 or B-3; otherwise, it corresponds to Case A-1, A-2 or A-3. In this figure, $\mathrm{C}_{\mathrm{Im}}^1$ and $\mathrm{C}_{\mathrm{Im}}^2$ are determined as $\mathrm{C}_{\mathrm{Im}}^{1,2} = \phi_\theta^{\mathrm{Im}}(\omega_I^{1,2})$ where $\omega_I^{1,2} = \pm[(b - c)/ab]^{\frac{1}{2}} \in \mathbb{R}$. On the other hand, $\mathrm{C}_{\mathrm{Re}}^1$ and $\mathrm{C}_{\mathrm{Re}}^2$ are determined as $\mathrm{C}_{\mathrm{Re}}^{1,2} = \phi_\theta^{\mathrm{Re}}(\omega_R^{1,2})$ where

$$(\omega_R^{1,2})^2 = \frac{(2a + c - 1) \pm [c^2 - 2(2a - 2b + c) + 1]^{1/2}}{2(a^2 + ac - b)} \in \mathbb{R}.$$

In the following, the θ-directional Lypunov $\mathcal{D}$-stabilization problem for the above multi-agent dynamical systems is considered.

7.2 GKYP lemma based pursuit formation $\mathcal{D}$-stabilization

In this subsection, the special case of the θ-directional pursuit formation $\mathcal{D}$-stabilization scheme developed in Section 6.1 is presented to clearly show its distinctive features. Consider the following θ-directional Lyapunov $\mathcal{D}$-stabilization problem:
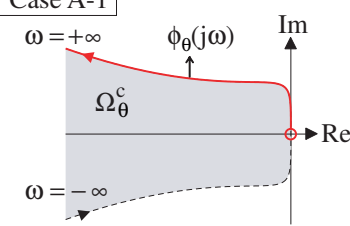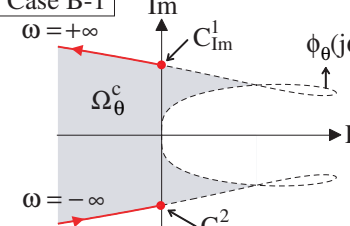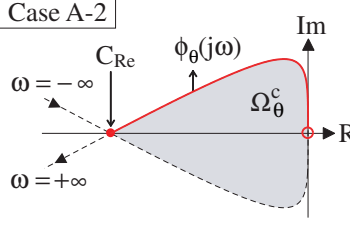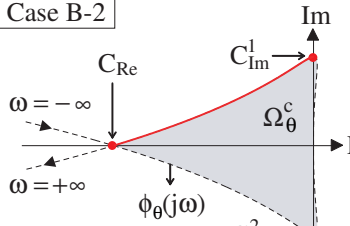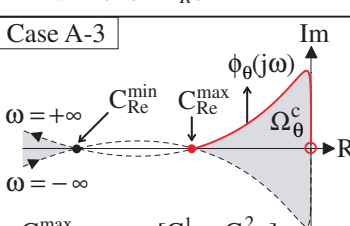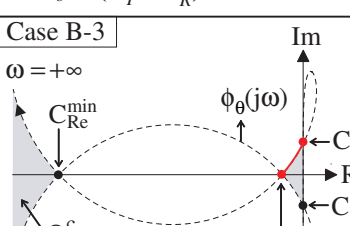
Conditions	$0 < b \leq c$	$b > c,\ b > 0$
$(\omega_R^{1,2})^2 \notin \mathbf{R}_+$	**Case A-1** $\omega = +\infty$, $\phi_\theta(j\omega)$, Im, Ω_θ^c, Re, $\omega = -\infty$	**Case B-1** $\omega = +\infty$, Im, C_{Im}^1, $\phi_\theta(j\omega)$, Ω_θ^c, Re, $\omega = -\infty$, C_{Im}^2
	Frequency range: $\omega_\varepsilon \leq \omega \leq \omega_\infty$ $$\Psi = \begin{bmatrix} -1 & j\omega_o \\ -j\omega_o & -\omega_\varepsilon\omega_\infty \end{bmatrix}$$ $\omega_o := (\omega_\varepsilon + \omega_\infty)/2$	Frequency range: $|\omega| \geq \omega_I^1$ $$\Psi = \begin{bmatrix} 1 & 0 \\ 0 & -(\omega_I^1)^2 \end{bmatrix}$$
$\begin{bmatrix} (\omega_R^1)^2 \in \mathbf{R}_+ \\ (\omega_R^2)^2 \notin \mathbf{R}_+ \end{bmatrix}$ or $\begin{bmatrix} (\omega_R^1)^2 \notin \mathbf{R}_+ \\ (\omega_R^2)^2 \in \mathbf{R}_+ \end{bmatrix}$	**Case A-2** C_{Re}, $\phi_\theta(j\omega)$, Im, $\omega = -\infty$, Ω_θ^c, Re, $\omega = +\infty$. $C_{Re} := C_{Re}^1$ or C_{Re}^2, $\omega_R := \omega_R^1$ or ω_R^2	**Case B-2** C_{Re}, C_{Im}^1, Im, $\omega = -\infty$, Ω_θ^c, Re, $\omega = +\infty$, $\phi_\theta(j\omega)$, C_{Im}^2
	Frequency range: $\omega_\varepsilon \leq \omega \leq \omega_R$ $$\Psi = \begin{bmatrix} -1 & j\omega_o \\ -j\omega_o & -\omega_\varepsilon\omega_R \end{bmatrix},\ \omega_R > 0$$ $\omega_o := (\omega_\varepsilon + \omega_R)/2$	Frequency range: $\omega_I^1 \leq \omega \leq \omega_R$ $$\Psi = \begin{bmatrix} -1 & j\omega_o \\ -j\omega_o & -\omega_I^1\omega_R \end{bmatrix},\ \omega_R > 0$$ $\omega_o := (\omega_I^1 + \omega_R)/2$
$(\omega_R^{1,2})^2 \in \mathbf{R}_+$	**Case A-3** Im, C_{Re}^{min}, C_{Re}^{max}, $\phi_\theta(j\omega)$, Ω_θ^c, $\omega = +\infty$, Re, $\omega = -\infty$. $C_{Re}^{max} := \max[C_{Re}^1, C_{Re}^2]$ $C_{Re}^{min} := \min[C_{Re}^1, C_{Re}^2]$	**Case B-3** $\omega = +\infty$, Im, C_{Re}^{min}, $\phi_\theta(j\omega)$, C_{Im}^1, Re, C_{Im}^2, Ω_θ^c, C_{Re}^{max}, $\omega = -\infty$
	Frequency range: $\omega_\varepsilon \leq \omega \leq \omega_R^{max}$ $$\Psi = \begin{bmatrix} -1 & j\omega_o \\ -j\omega_o & -\omega_\varepsilon\omega_R^{max} \end{bmatrix},\ \omega_R^{max} > 0$$ $\omega_o := (\omega_\varepsilon + \omega_R^{max})/2$	Frequency range: $\omega_I^1 < \omega < \omega_R^{max}$ $$\Psi = \begin{bmatrix} -1 & j\omega_o \\ -j\omega_o & -\omega_I^1\omega_R^{max} \end{bmatrix},\ \omega_R^{max} > 0$$ $\omega_o := (\omega_I^1 + \omega_R^{max})/2$

Figure 11: PID controller case: Six types of ranges of ω and the corresponding Ψ

Problem S1': For given $p_\theta(s)$, $c_\theta(s)$ (i.e., a, b and c in (48) are given) and $\varphi = \pi/2$, how to find the upper bound $k_{\max_\theta}$ of a connectivity gain $k_\theta (> 0)$, which guarantees nonzero $n-1$ eigenvalues of A_θ with $k_\theta (\leq k_{\max_\theta})$ belong to Ω_θ^c depicted in Figure 11.

Now, one can easily find from Figure 4 that if a given k_θ satisfies that

$$(\phi_\theta(j\omega) + k_\theta)^*(\phi_\theta(j\omega) + k_\theta) > k_\theta^2, \ \forall \omega \in \mathbb{R}\backslash\{0\}, \tag{51}$$

then nonzero $n-1$ eigenvalues λ_i ($i = 2, 3, \cdots, n$) of A_θ are placed in the domain Ω_θ^c. Then, similarly to (37), it is equivalent to (51) that

$$\begin{bmatrix} h_\theta(j\omega) \\ 1 \end{bmatrix}^* \Pi \begin{bmatrix} h_\theta(j\omega) \\ 1 \end{bmatrix} < 0, \ \Pi := \begin{bmatrix} 0 & -k_\theta \\ -k_\theta & -1 \end{bmatrix} \tag{52}$$

for $\forall \omega \in \mathbb{R}\backslash\{0\}$. Note that $h_\theta(s)$ in (52) is proper as shown in (48), and thus has the state-space realization given by $h_\theta(s) \sim (A_{h_\theta}, B_{h_\theta}, C_{h_\theta}, D_{h_\theta})$ in (39). For the above problem, the frequency-domain inequality (FDI) specification (52) can easily be checked by using the GKYP lemma, which transforms a FDI in a finite (or semi-infinite) frequency range into a set of LMIs as mentioned in the optimization problem of Section 6.1. It means that checking the FDI in (52) within a given frequency range specified in Figure 11 can be converted to searching for matrices $P \in \mathbf{H}_n$ and $Q \in \mathbf{H}_n$ satisfying the LMIs in (43). In this problem setting, $\Psi \in \mathbf{H}_2$ is set as defined in Figure 11 where ω_ϵ and ω_∞ denote, respectively, infinitesimally small positive real number and sufficiently large positive real number (these are design variables). Also, $\omega_R^{\max}$ and $\omega_R^{\min}$ denote, respectively, the frequencies corresponding to $\text{C}_{\text{Re}}^{\max}$ and $\text{C}_{\text{Re}}^{\min}$. On the other hand, $\Gamma \in \mathbf{H}_2$ is set as $\Gamma := \begin{bmatrix} 0 & 1 \\ 1 & 0 \end{bmatrix}$ since the continuous-time setting is considered in this paper [4].

Based on the above results, the upper bound $k_{\max_\theta}$ of a connectivity gain $k_\theta (> 0)$ is readily obtained by just solving the following constrained optimization:

Optimization problem for Problem S1': For given $p_\theta(s)$ and $c_\theta(s)$, solve

$$k_{\max_\theta} := \arg \max_{k_\theta, P \in \mathbf{H}_n, Q \in \mathbf{H}_n} k_\theta \tag{53}$$

subject to $k_\theta > 0$ and LMI constraints in (43) with $\Gamma := \begin{bmatrix} 0 & 1 \\ 1 & 0 \end{bmatrix}$ and $\Psi \in \mathbf{H}_2$ defined in Figure 11.
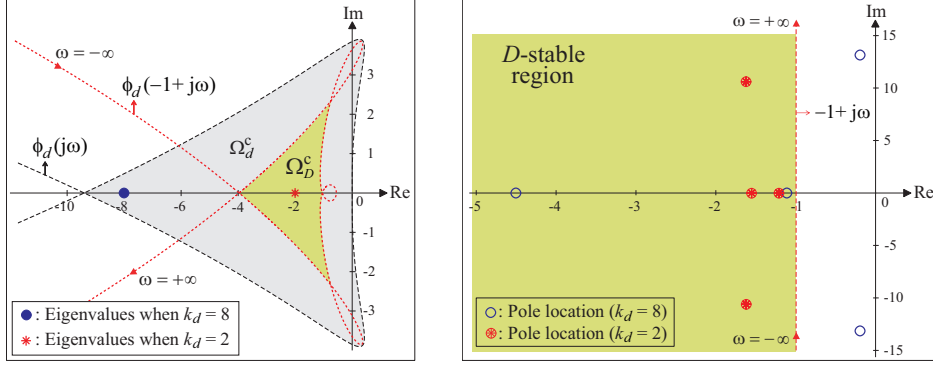
(a) The images of $\phi_d(j\omega)$, $\phi_d(-1+j\omega)$, and the corresponding domains Ω_d^c, Ω_D^c.

(b) The pole locations of $\mathcal{H}_d(s)$ with two different values of k_d.

Figure 12: Example: The d-directional formation stabilization.

Remark 1 *The d- or α-directional stabilization can be easily achieved comparing to the θ-directional stabilization problem, since A_d in (13) and A_α in (14) have n multiple eigenvalues at $(-k_d + j0)$ and $(-k_\alpha + j0)$, respectively. For example, if we want to place the poles of $\mathcal{H}_d(s)$ with $p_d(s) = 1/(s(s-1))$ and $c_d(s) = 12\,(1 + 1/3s + s/4)$ at the predesignated $\mathcal{D}$-stable region in Figure 12(b), then $(-k_d + j0)$ should belong to the domain Ω_D^c defined as*

$$\Omega_D := \phi_d(\mathbb{C}_D), \quad \Omega_D^c := \mathbb{C}\backslash\Omega_D, \quad \phi_d(s) = \frac{\frac{1}{108}s^4 + \frac{1}{18}s^3 + s^2 + s}{\frac{1}{12}s^2 + s + 1} \quad (54)$$

where $\mathbb{C}_D = \{s \in \mathbb{C} : \text{Re}[s] \geq -1\}$ (see Figure 12(a)). The pole locations for $k_d = 8$ and $k_d = 2$ are illustrated in Figure 12(b).

In the following section, we present an optimization-based design method for dynamic agent's local controller.

8 Pursuit formation stabilization: Local PD controller design

In this section, it is assumed that only an agent's dynamics $p_\theta(s)$ in (44) is given a priori. Then, we consider how to design the PD controller

$$c_\theta(s) = \hat{k}_p(1 + \hat{t}_d s), \quad \hat{k}_p > 0, \quad \hat{t}_d > 0, \quad (55)$$

so that we can get the largest value of a connectivity gain k_θ which guarantees the formation stability. In the following, we will show that the above problem can be reduced to a constrained polynomial optimization problem.

25

Problem S2: For a given $p_\theta(s)$ in (44), find the PD controller's gains $\hat{k}_p$ and $\hat{t}_d$ in (55), and its corresponding upper bound $k_{\max_\theta}$ of a connectivity gain which satisfies the following global pursuit formation Lypunov $\mathcal{D}$-stability condition: all nonzero poles of $\mathcal{H}_\theta(s)$ belong to the $\mathcal{D}$-stable region, D_{LHP}, defined in Figure 4.

Before we proceed, the generalized frequency variable $\phi_\theta(s)(= 1/h_\theta(s) = s/g_\theta(s))$ is defined from (44) and (55) as

$$\phi_\theta(s) = \frac{\hat{a}s^3 + \hat{b}s^2 + s}{s + 1}, \quad \hat{a} := \frac{1}{\zeta \hat{k}_p \hat{t}_d^2}(> 0), \quad \hat{b} := \frac{\xi}{\zeta \hat{k}_p \hat{t}_d} + 1. \quad (56)$$

Then, in order to develop an optimization problem for the above problem, we first consider the following inequality condition which is derived from (51) and (56):

$$L(\omega) := -2\mathrm{Re}[h_\theta(j\omega)] = \frac{2(\hat{a}\omega^2 + \hat{b} - 1)}{\hat{a}^2\omega^4 + (\hat{b}^2 - 2\hat{a})\omega^2 + 1} < \frac{1}{k_\theta} \quad (57)$$

for $\forall \omega \in \mathbb{R} \backslash \{0\}$. The condition (57) implies that if a given k_θ^{-1} is bigger than the maximum value of $L(\omega)$ (except at $\omega = 0$), then nonzero $n-1$ eigenvalues λ_i $(i = 2, 3, \cdots, n)$ of A_θ are placed in the domain Ω_θ^c defined via (56) as shown in Figure 14 (refer to [5]). From the above observations, the following key result that specifies the maximum permissible limit of a gain $k_\theta(> 0)$ is obtained, which is an alternative algebraic formation stabilization method.

Theorem 3 *Let $L_{\max_0}$ and $L_{\max_1}$ be defined, respectively, as*

$$L_{\max_1}(\hat{a}, \hat{b}) := \frac{2(\hat{a}\hat{\omega} + \hat{b} - 1)}{\hat{a}^2\hat{\omega}^2 + (\hat{b}^2 - 2\hat{a})\hat{\omega} + 1}, \quad L_{\max_0}(\hat{b}) := 2(\hat{b} - 1),$$

where

$$\hat{\omega} := \frac{1 - \hat{b}}{\hat{a}} + \frac{\hat{b}}{\hat{a}^2}\sqrt{\hat{a}(\hat{a} - \hat{b} + 1)}. \quad (58)$$

Suppose that for given $\hat{a}$ and $\hat{b}$, an connectivity gain $k_\theta(> 0)$ in (10) satisfies the following condition:

(I) $k_\theta < L_{\max_1}^{-1}(\hat{a}, \hat{b})$, if $\hat{\omega}$ is a positive real number and $L_{\max_1}(\hat{a}, \hat{b}) \geq L_{\max_0}(\hat{b})$,

(II) $k_\theta \leq L_{\max_0}^{-1}(\hat{b})$, otherwise.

Then, nonzero $n - 1$ eigenvalues λ_i $(i = 2, 3, \cdots, n)$ of A_θ are placed in the domain Ω_θ^c.
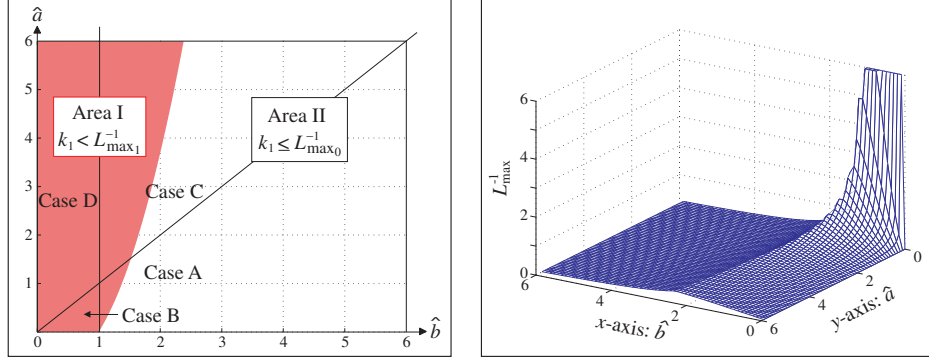
(a) Areas I and II determined via Theorem 3 (I) and (II)

(b) The plot of $L_{\max}^{-1}$ in the $\hat{a}$-$\hat{b}$ plane

Figure 13: Areas I-II and the plot of $L_{\max}^{-1}$.

The region where the constraint condition in Theorem 3 (I) is satisfied is illustrated in Figure 13(a) (Area I). It means that if given $\hat{a}$ and $\hat{b}$ of (56) exist in Area I, then the maximum value of k_θ should be determined by $k_\theta < L_{\max_1}^{-1}$. On the other hand, if $\hat{a}$ and $\hat{b}$ exist in Area II, then $k_\theta \leq L_{\max_0}^{-1}$. Figure 13(b) illustrates the plot of $L_{\max}^{-1}$ which is set as $L_{\max}^{-1} = L_{\max_1}^{-1}$ in Area I and $L_{\max}^{-1} = L_{\max_0}^{-1}$ in Area II.

Based on the results in Theorem 3, the following optimization-based agent design method can easily be formulated:

Optimization problem for Problem S2: In order to determine the system parameters $\hat{a}$ and $\hat{b}$ of $g_\theta(s)$ in Area I, solve

$$\min_{(\hat{a},\hat{b})\in\mathcal{S}} L_{\max_1}^{-1}(\hat{a},\hat{b}) \tag{59}$$

subject to

$$\hat{w} \text{ is a positive real number} \tag{60}$$
$$L_{\max_1}(\hat{a},\hat{b}) \geq L_{\max_0}(\hat{b}) \tag{61}$$

where an agent's dynamics in the form of (44) is given, and $\mathcal{S}$ denotes a predefined set of $\hat{a}$ and $\hat{b}$. Then, the PD controller's gains $\hat{k}_p > 0$ and $\hat{t}_d > 0$ in (55) are obtained from $\hat{a}^* = 1/(\zeta\hat{k}_p\hat{t}_d^2)$ and $\hat{b}^* = \xi/(\zeta\hat{k}_p\hat{t}_d) + 1$ where $\hat{a}^*$ and $\hat{b}^*$ denote optimal values. Further, the maximum of a connectivity gain k_θ is obtained as $L_{\max_1}^{-1}(\hat{a}^*,\hat{b}^*)$.

27

Conditions	$\hat{b} > 1$	$0 < \hat{b} \leq 1$
$0 < \hat{a} < \hat{b}$	**Case A** — (diagram: $\omega = +\infty$, $\phi_\theta(j\omega)$, Ω_θ^c, $\omega = -\infty$, Im, Re)	**Case B** — (diagram: $\omega = +\infty$, $\phi_\theta(j\omega)$, Ω_θ^c, C_{Im}^1, C_{Im}^2, $\omega = -\infty$, Im, Re)
	Frequency range: $\omega_\varepsilon \leq \omega \leq \omega_\infty$ $$\Psi = \begin{bmatrix} -1 & j\omega_o \\ -j\omega_o & -\omega_\varepsilon\omega_\infty \end{bmatrix}$$ $\omega_o := (\omega_\varepsilon + \omega_\infty)/2$	Frequency range: $|\omega| \geq \omega_I^1$ $$\Psi = \begin{bmatrix} 1 & 0 \\ 0 & -(\omega_I^1)^2 \end{bmatrix}$$
$\hat{a} \geq \hat{b} > 0$	**Case C** — (diagram: $\omega = -\infty$, C_{Re}, $\phi_\theta(j\omega)$, Ω_θ^c, $\omega = +\infty$, Im, Re)	**Case D** — (diagram: $\omega = -\infty$, C_{Re}, C_{Im}^1, Ω_θ^c, $\omega = +\infty$, $\phi_\theta(j\omega)$, C_{Im}^2, Im, Re)
	Frequency range: $\omega_\varepsilon \leq \omega \leq \omega_R$ $$\Psi = \begin{bmatrix} -1 & j\omega_o \\ -j\omega_o & -\omega_\varepsilon\omega_R \end{bmatrix}, \ \omega_R > 0$$ $\omega_o := (\omega_\varepsilon + \omega_R)/2$	Frequency range: $\omega_I^1 \leq \omega \leq \omega_R$ $$\Psi = \begin{bmatrix} -1 & j\omega_o \\ -j\omega_o & -\omega_I^1\omega_R \end{bmatrix}, \ \omega_R > 0$$ $\omega_o := (\omega_I^1 + \omega_R)/2$

Figure 14: PD controller case: Four types of ranges of ω and the corresponding Ψ

On the other hand, once the system parameters $\hat{a}^*$ and $\hat{b}^*$ of $h_\theta(s)$ which maximize a connectivity gain are determined via the above optimization problem, then it is possible to apply the $\mathcal{D}$-stabilization strategy presented in Section 7 to find a $\mathcal{D}$-stabilizing connectivity gain k_θ. In this case, $\Psi \in \mathbf{H}_2$ is set as defined in Figure 14 where

$$\omega_I^{1,2} = \pm\left(\frac{1-\hat{b}}{\hat{a}}\right)^{1/2} \in \mathbb{R}, \quad \omega_R^{1,2} = \pm\frac{1}{(\hat{a}-\hat{b})^{1/2}} \in \mathbb{R}. \tag{62}$$

Note that, if we intend to design $\hat{a}$ and $\hat{b}$ in Area II, these values can be easily determined from the condition presented in Theorem 3 (II).

It is also important to note that one can add additional constraint condition denoted by $\mathcal{S}$ in the above optimization problem. For example, in the
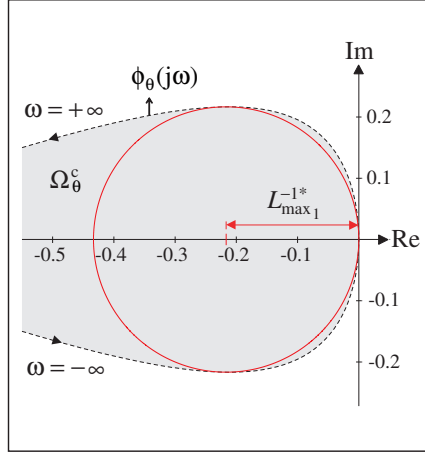
Figure 15: The simulation result of Example 3: The image of $\phi_\theta(j\omega)$ and the circle of radius 0.2167

following example, the additional constraint conditions such that

(c1) all the poles of $g_\theta(s)$ are located in a predesignated region in the complex plane; i.e., the $\mathcal{D}$-stabilization problem for each agent,

(c2) the predefined ranges of $\hat{a}$ and $\hat{b}$, which are set based on the desirable ranges of $\hat{k}_p$ and $\hat{t}_d$,

are considered. In order to derive a numerical formulation for the constraint condition (c1), we introduce the following notations: let $\lambda_i(g_\theta(s))$ denote the ith pole of the system $g_\theta(s)$, and $\lambda_{\max}(g_\theta(s))$ be the pole whose real part is greater than those of other poles, i.e.,

$$\mathrm{Re}[\lambda_{\max}(g_\theta(s))] = \max_i\{\mathrm{Re}[\lambda_i(g_\theta(s))], \ \forall i\}.$$

The above-mentioned constrained polynomial optimization problem for "Problem S2" subject to additional constraints (c1) and (c2) can easily be solved through the constrained particle swarm optimization scheme [12], which will be verified in the following example.

Example 3 *Suppose that agent's dynamics is given as $p_\theta = 1/s(s+2)$. We here consider the following two additional constraints as well as (60)-(61):*

$$\mathrm{Re}[\lambda_{\max}(\mathrm{g}_\theta(\mathrm{s}))] \leq -0.25, \tag{63}$$

$$3.0 \leq \hat{a} \leq 6.0, \quad 1.1 \leq \hat{b} \leq 2.5. \tag{64}$$

Then, $\hat{a}$ and $\hat{b}$ in (56) can readily be obtained by solving the optimization problem (59) subject to (60)-(64). The optimization problem is solved via constrained PSO method [12], and then we obtain the minimum of $L_{\max_1}^{-1}$ as $L_{\max_1}^{-1}(\hat{a}^*, \hat{b}^*) = 0.2167$ where $\hat{a}^* = 5$ and $\hat{b}^* = 2.5$. Therefore, we have

$\hat{k}_p = 8.8889$ and $\hat{t}_d = 0.15$. The image of $\phi_\theta(j\omega)$ with the above $\hat{a}^*$ and $\hat{b}^*$ is illustrated in Figure 15, where the radius of circle is 0.2167. From the above results, we can easily see that if k_θ is set as $0 < k_\theta < L_{\max_1}^{-1*} = 0.2167$, the global pursuit formation Lypunov $\mathcal{D}-$stability presented in "Problem S2" is guaranteed.

9   Conclusion

In this paper, we have presented novel formation stability analysis and formation stabilization schemes for a distributed cooperative control based on a cyclic pursuit strategy. As for the formation stability analysis, we introduced a $\mathcal{D}$-stability problem in multi-agent dynamical systems, and then developed a simple diagrammatic pursuit formation stability criterion. Then, as for the formation stabilization problem when agent's dynamics and its local controller are given, we developed an optimization problem subject to LMI constraints to maximize the connectivity gain of a cyclic pursuit based on-line path generator, which satisfies not only a global formation stability condition but also a required multi-agent system's performance specification. In this case, the LMIs are derived based on the generalized Kalman-Yakubovich-Popov (GKYP) lemma. Then, in order to clearly show its distinctive features, we considered the special case of a pursuit formation stabilization scheme for a class of multi-agent systems where each agent is modeled as a second-order system and is locally stabilized by the PID controller. Finally, a constrained polynomial optimization problem was developed in order to design agent's local PD controller parameters guaranteeing that a given connectivity gain becomes the maximum one satisfying the global formation stability condition for a class of dynamic agents given a priori. The effectiveness of the proposed stabilization schemes was verified through simulation examples.

References

[1] P. J. Davis. *Circulant matrices*. John Wiley and Sons, 1979.

[2] J. A. Fax and R. M. Murray. Information flow and cooperative control of vehicle formations. *IEEE Transactions on Automatic Control*, 49(9):1465–1476, 2004.

[3] S. Hara, T. Hayakawa, and H. Sugata. Stability analysis of linear systems with generalized frequency variables and its application to formation control. In *Proceedings of the 46th IEEE Conference on Decision and Control*, pages 1459–1466, New Orleans, LA, USA, 2007.

[4] S. Hara, T. Iwasaki, and D. Shiokata. Robust PID control using generalized KYP synthesis: direct open-loop shaping in multiple frequency ranges. *IEEE Control Systems Magazine*, 26(1):80–91, 2006.

[5] S. Hara, T.-H. Kim, and Y. Hori. Distributed formation control for target-enclosing operation by multiple dynamic agents based on a cyclic pursuit strategy. Technical Report METR 2007-62, The University of Tokyo, http://www.keisu.t.u-tokyo.ac.jp/research/techrep/index.html, 2007.

[6] T. Iwasaki and S. Hara. Generalized KYP lemma: Unified frequency domain inequalities with design applications. *IEEE Transactions on Automatic Control*, 50(1):41–59, 2004.

[7] T.-H. Kim, S. Hara, and Y. Hori. Distributed cyclic pursuit formation control for target-enclosing operations by multi-agent dynamical systems. *International Journal of Control*, 2009. (submitted).

[8] T.-H. Kim and T. Sugie. Cooperative control for target-capturing task based on a cyclic pursuit strategy. *Automatica*, 43(8):1426–1431, 2007.

[9] K. Kobayashi, K. Otsubo, and S. Hosoe. Design of decentralized capturing behavior by multiple robots. In *IEEE Workshop on Distributed Intelligent Systems: Collective Intelligence and its applications*, pages 463–468, 2006.

[10] J. A. Marshall, M. E. Broucke, and B. A. Francis. Formations of vehicles in cyclic pursuit. *IEEE Transactions on Automatic Control*, 49(11):1963–1974, 2004.

[11] J. A. Marshall, M. E. Broucke, and B. A. Francis. Pursuit formations of unicycles. *Automatica*, 42:3–12, 2006.

[12] I. Maruta, T.-H. Kim, and T. Sugie. Fixed-structure H_∞ controller synthesis: A meta-heuristic approach using simple constrained particle swarm optimization. *Automatica*, 45(2):553–559, 2009.

[13] R. M. Murray. Recent research in cooperative control of multivehicle systems. *Transactions of the ASME Journal of Dynamic Systems, Measurement, and Control*, 129(9):571–583, 2007.

[14] R. Olfati-Saber, J. A. Fax, and R. M. Murray. Consensus and cooperation in networked multi-agent systems. *Proceedings of the IEEE*, 95(1):215–233, 2007.

[15] R. Sepulchre, D. A. Paley, and N. E. Leonard. Group coordination and cooperative control of steered particles in the plane. In *Group Coordination and Cooperative Control*, pages 217–232. Springer-Verlag: Lecture Notes in Control and Information Sciences, 2006.

A Lemma for the pole locations of $\mathcal{H}_\theta(s)$

The following lemma shows that the pole locations of large-scale system $\mathcal{H}_\theta(s)$ can be found by using $\phi_\theta(s)$ obtained from an agent's dynamics and A_θ obtained from a path generation law:

> **Lemma 1** *Consider a large-scale linear system $\mathcal{H}_\theta(s)$ in (15) and (17). The poles of $\mathcal{H}_\theta(s)$ are identical, including multiplicity, to the roots of $|\phi_\theta(s)I_n - A_\theta| = 0$.*

Proof From (15) and (17), the transfer function $\mathcal{H}_\theta(s)$ can be rewritten as

$$\mathcal{H}_\theta(s) = (\phi_\theta(s)I_n - A_\theta)^{-1}B_\theta. \tag{65}$$

Let $n(s)/d(s) := h_\theta(s)$ which is a irreducible fraction. Then, we have

$$\mathcal{H}_\theta(s) = n(s)\frac{\mathrm{adj}(d(s)I_n - n(s)A_\theta)}{|d(s)I_n - n(s)A_\theta|}B_\theta \tag{66}$$

where $\mathrm{adj}(\cdot)$ is a adjugate matrix. Since (A_θ, B_θ) is controllable, the poles of $\mathcal{H}_\theta(s)$ are identical, including multiplicity, to the roots of

$$|d(s)I_n - n(s)A_\theta| = 0. \tag{67}$$

Also, since $d(s)$ and $n(s)$ are irreducible polynomials, s_0 satisfying $n(s_0) = 0$ cannot be a root of (67). Therefore, the roots of (67) are identical to the roots of the following equation:

$$\left|\frac{d(s)}{n(s)}I_n - A_\theta\right| = |\phi_\theta(s)I_n - A_\theta| = 0. \tag{68}$$